

Article

An Amidochlorin-Based Colorimetric Fluorescent Probe for Selective Cu²⁺ Detection

Wenting Li [†], Guohua Zhu [†], Jinghua Li [†], Zhiqiang Wang ^{*} and Yingxue Jin ^{*}

Received: 5 December 2015 ; Accepted: 14 January 2016 ; Published: 18 January 2016
Academic Editors: Scott Reed and Marino Resendiz

Key Laboratory for Photonic and Electronic Bandgap Materials, Ministry of Education, College of Chemistry & Chemical Engineering, Harbin Normal University, Harbin 150025, China; m13039864430@163.com (W.L.); zhuguohua201@163.com (G.Z.); jyxprof@163.com (J.L.)

^{*} Correspondence: wzq70402@163.com (Z.W.); tgh.123@163.com (Y.J.); Tel.: +86-451-8806-0570 (Z.W.); +86-451-8806-0569 (Y.J.)

[†] These authors contributed equally to this work.

Abstract: The design and synthesis of selective and sensitive chemosensors for the quantification of environmentally and biologically important ionic species has attracted widespread attention. Amidochlorin p6 (ACP); an effective colorimetric and fluorescent probe for copper ions (Cu²⁺) in aqueous solution derived from methyl pheophorbide-a (MPa) was designed and synthesized. A remarkable color change from pale yellow to blue was easily observed by the naked eye upon addition of Cu²⁺; and a fluorescence quenching was also determined. The research of fluorescent quenching of ACP-Cu²⁺ complexation showed the detection limit was 7.5×10^{-8} mol/L; which suggested that ACP can act as a high sensitive probe for Cu²⁺ and can be used to quantitatively detect low levels of Cu²⁺ in aqueous solution. In aqueous solution the probe exhibits excellent selectivity and sensitivity toward Cu²⁺ ions over other metal ions (M = Zn²⁺; Ni²⁺; Ba²⁺; Ag⁺; Co²⁺; Na⁺; K⁺; Mg²⁺; Cd²⁺; Pb²⁺; Mn²⁺; Fe³⁺; and Ca²⁺). The obvious change from pale yellow to blue upon the addition of Cu²⁺ could make it a suitable “naked eye” indicator for Cu²⁺.

Keywords: fluorescent probe; copper ions; chlorophyll

1. Introduction

The design and synthesis of selective and sensitive chemosensors for the quantification of environmentally and biologically important ionic species has attracted widespread attention [1]. Among ionic species, copper is one of the important pollution sources [2]. As a common heavy metal existing widely in Nature and all living organisms, an appropriate amount of copper ion is essential to living organisms because it is a key constituent of the respiratory enzyme complex cytochrome c oxidase [3]. However, excess copper ion may cause physical discomfort and sometimes life-threatening illness [4–7]. Therefore the determination of heavy metal content in living organisms and the environment is particularly important.

Because chromo- or fluoroionophores are highly effective for these determinations, given their easy handling and the simple equipment required, effort has been expended to develop optical chemosensors that selectively respond to the Cu²⁺ ion. Various methods have been developed in the past decades to determine Cu²⁺ ion content, such as spectrophotometric [8–10], electrochemical (EM) [11–13], inductively coupled plasma atomic emission spectrometric (ICP-AES) [14–17], atomic absorption spectroscopic (AAS) [18,19] and fluorescence methods [20–22]. Among them, the fluorescence method utilizes a specific chemical reaction between dosimeter molecules and the target species to form a fluorescent or colored product. Thus, high selectivity toward the probe is an advantage of chemodosimeters, making them useful for detecting Cu²⁺ ions. Meanwhile, as

1 mM solutions of metallic ions were prepared by dissolving the appropriate salts in doubly distilled water, respectively, and then diluting to a lower concentration of 10 μM . Meanwhile, a stock 1 mM solution of **ACP** was also prepared in ethanol, and then diluted to a lower concentration of 10 μM . In brief, to a 10 mL volumetric flask, 100 μL of the stock solution (1 mM) of **ACP** was added, followed by addition of 100 μL of different metal ions stock solutions, the mixtures were diluted to lower concentrations by addition of 50% ethanol (*v/v*) solution. As a control, the same procedure was performed but in the absence of Cu^{2+} .

2.3. Spectral Titration of **ACP** with Cu^{2+}

Copper is a quenching metal ion and the coordination of **ACP** with Cu^{2+} would quench the fluorescence of **ACP**. The UV-Vis and fluorescence titration experiments of **ACP** with Cu^{2+} were performed in 50% ethanol (*v/v*) solution. Figure 1a shows the UV-visible absorption spectrum of **ACP**. **ACP** absorbs throughout the ultraviolet region into the visible region between about 400 and 800 nm with four peaks: a strong Soret absorption peak at 399 nm, two weak absorption peaks at 499 nm and 605.5 nm, and a Qy peak at 660.5 nm. The absorption of **ACP** is highly affected by the presence of Cu^{2+} ions. Upon addition of Cu^{2+} ions, the absorption intensity of Soret peak at 399 nm decreased with a little red shift, and the peak at 499 nm also decreased, with no peak shift. Meanwhile, the Qy peak gradually reduced in intensity with the formation of a new absorption peak at about 632 nm and with the formation of an isosbestic point at 652 nm. When the concentration of Cu^{2+} increased to the same level as **ACP**, the Qy peak disappeared yet the absorption intensity at 632 nm reached a maximum. The change of **ACP** absorption spectra demonstrated the complexation between **ACP** and Cu^{2+} . The value of the shift is indicative of the degree of the interaction between the fluorophore and the bound Cu^{2+} . To study the binding stoichiometry of **ACP** and Cu^{2+} , a Job's plot experiment was carried out by using the UV-Vis absorbance spectrum at 632 nm. Keeping the sum of the initial concentration of Cu^{2+} and **ACP** at 10 μM , increasing the concentration of Cu^{2+} from 0 to 1. The maximum absorbance occurred when the $[\text{Cu}^{2+}]/([\text{ACP}]+[\text{Cu}^{2+}])$ reached at 0.5.

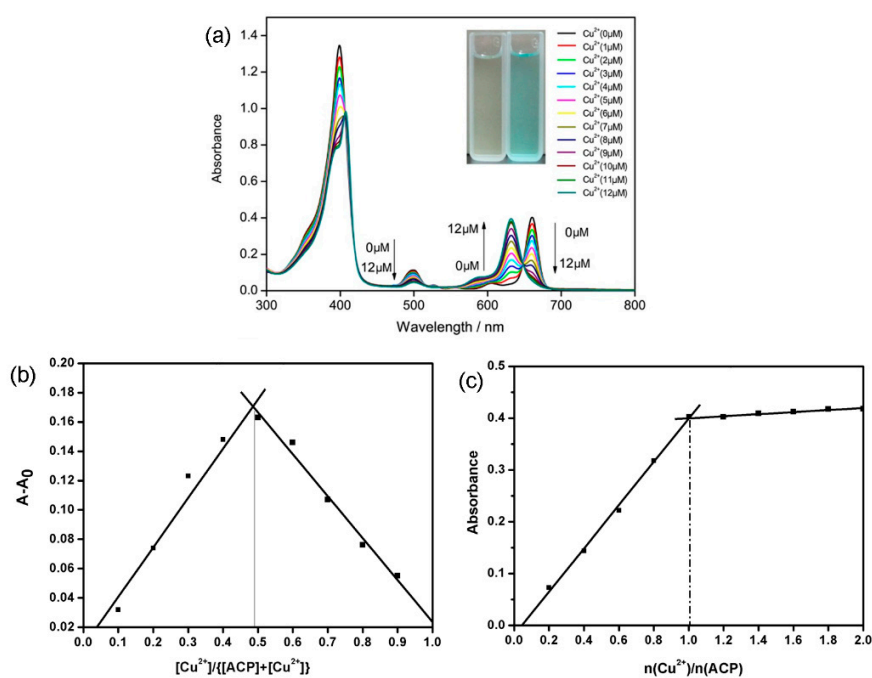


Figure 1. (a) The absorption spectrum of **ACP** in water/ethanol (*v/v* = 50/50) solution (10 μM) with added Cu^{2+} ; (b) Job's plot according to the method for continuous variations (the total concentration of **ACP** and Cu^{2+} is 10 μM). The absorbance was measured at 632 nm; (c) Mole ratio plot for stoichiometric ratio between **ACP** (10 μM each) and Cu^{2+} .

This observation indicates that **ACP** and Cu^{2+} formed at 1:1 ratio complex. In order to verify this, the mole ratio plot for stoichiometric ratio between **ACP** (10 μM each) and Cu^{2+} was measured. As can be seen from Figure 1c, the molar ratio of **ACP** to Cu^{2+} was 1:1.

The fluorescence titration of Cu^{2+} was carried out using a solution of 10 μM **ACP** in ethanol, using 412 nm as excitation wavelength. As illustrated in Figure 2a, the fluorescence intensity of **ACP** decreases with increasing concentration of Cu^{2+} , which constitutes the basis for the determination of Cu^{2+} with the fluorescent probe proposed in this paper. Moreover, it can be seen from Figure 2b that the fluorescence intensity at 632 nm showed a linear quenching with the increasing addition of Cu^{2+} . The fluorescent response of **ACP** toward Cu^{2+} was calculated to cover a linear range from 1 to 10 μM . The linear equation was $y = -45.66x + 546.27$ ($R^2 = 0.999$), where y is the fluorescence intensity at 668 nm measured at a given Cu^{2+} concentration and x is the concentration of Cu^{2+} added. The detection limit of Cu^{2+} is 7.5×10^{-8} mol/L, which is lower than the limit of Cu^{2+} in drinking water ($\sim 20 \mu\text{M}$) demanded by U.S. Environmental Protection Agency. This result showed that **ACP** is sensitive enough to monitor the concentration of Cu^{2+} in drinking water.

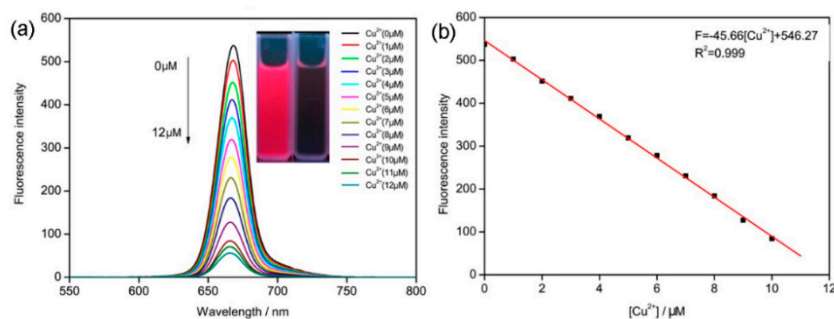


Figure 2. (a) Fluorescence spectra of $[\text{ACP-Cu}^{2+}]$ with emission wavelength 668 nm; (b) The relation between **ACP** fluorescence intensity and the concentration of Cu^{2+} .

2.4. Selectivity and Interference Studies

Selectivity is a very important parameter to evaluate the performance of a probe. Development of chemosensors with “naked eye” capability has an advantage over traditional fluorescence sensors because they do not need cumbersome labor and a sophisticated instruments [33]. The selectivity of **ACP** toward Cu^{2+} and the interference of a number of common ions with the determination of Cu^{2+} were investigated. The experiments were carried out by fixing the concentration of Cu^{2+} at 10 μM and then recording the change of the UV-Vis absorbance and fluorescence intensity before and after adding the interferent into the Cu^{2+} solution (Figure 3). In the presence of other tested metal ions (Zn^{2+} , Ni^{2+} , Ba^{2+} , Ag^+ , Co^{2+} , Na^+ , K^+ , Mg^{2+} , Cd^{2+} , Pd^{2+} , Mn^{2+} , Fe^{3+} , and Ca^{2+}), the UV-Vis absorbance spectra showed almost no obvious change relative to the free ligand **ACP**, and the absorbance of **ACP** was only slightly influenced by the addition of other ions (Figure 3a). When 1 equiv. of Cu^{2+} and selected metal ions (10 μM) was added into the solution of **ACP** (10 μM), many of the investigated metal ions do not interfere with detection of Cu^{2+} . The data in Figure 4 clearly reveals that the addition of other common metal ions can hardly affect the fluorescence response of **ACP** towards Cu^{2+} . There are only slight interfering effects of Mg^{2+} and Cd^{2+} . These results clearly suggest that the probe **ACP** shows a high anti-interference ability against other potentially coexisting metal ions.

Furthermore, upon addition of the same amount of the various metal ions, respectively, only Cu^{2+} induced a striking color change from pale yellow to blue, as observed by the naked eye (Figure 3a). Those observations indicate that **ACP** has a high selectivity to Cu^{2+} and can be a good colorimetric sensor for Cu^{2+} ions. Moreover, upon addition of Cu^{2+} and selected metal ions (10 μM), only Cu^{2+} showed distinct quenching (Figure 3a,b), which suggested that **ACP** can be a selective fluorescent sensor for Cu^{2+} ions. It’s worth mentioning that upon addition of Cu^{2+} , the color of **ACP** changed

much faster than PPME that previously reported in the literature [31]. In brief, our proposed probe shows extraordinary selectivity to Cu^{2+} and could meet the selectivity requirements for biomedical and environmental applications.

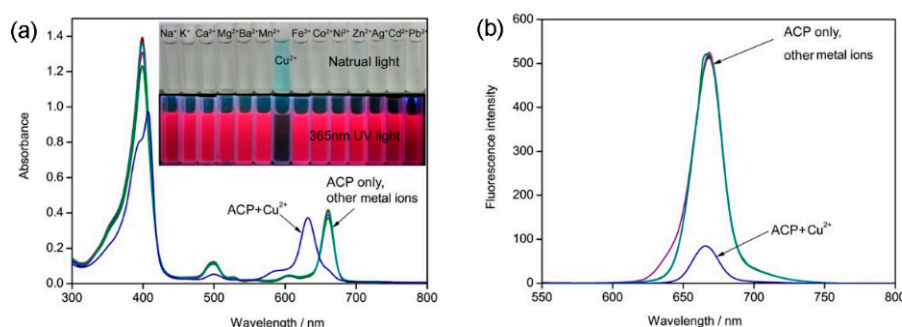


Figure 3. (a) UV-Vis absorption and (b) fluorescence emission spectra of ACP (10 μM) upon addition of various metal ions (10 μM) in water/ethanol ($v/v = 50/50$) solution. The color changes of ACP (10 μM) upon addition 1 equiv. of various metal ions under natural light and UV-Vis are also displayed.

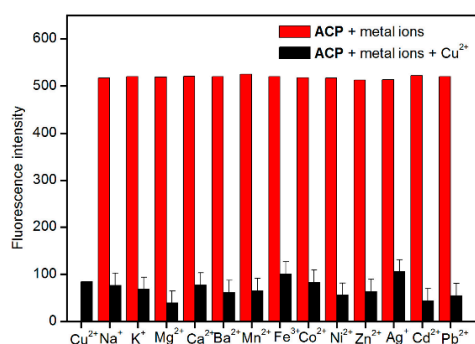


Figure 4. The relative fluorescence intensity diagram of ACP (10 μM) to different metal ions (1 equiv.). Excitation was at 412 nm, and emission was at 668 nm.

2.5. Spike and Recovery Test

Spike and recovery test was conducted in tap water to examine whether there is any positive or negative interference in real drinking water samples. We first examined the effect of tap water on the fluorescence stability and found no quenching effect. The local tap water was filtered first through filter paper to remove any insoluble suspended solids. The recovery study was carried out on a mixture of water and ethanol (1:1, v/v) which was spiked with 2, 5 and 8 μM Cu^{2+} . Each experiment was done in quintuplicate and the average was presented with relative standard deviation. The contents of Cu^{2+} were recovered using the linear equation obtained in Figure 3. The analysis results for the sample with spiked Cu^{2+} were given in Table 1. The result showed that the method had a good recovery at the concentration test, suggesting no serious positive or negative interferences for selectively and sensitively determining copper(II) ion in real water samples.

Table 1. Recovery test of Cu^{2+} in tap water ¹.

Tap Water Sample	Cu^{2+} Added (μM)	Cu^{2+} Found (μM)	RSD (% , $n = 5$)	Recovery (%)
Sample 1	2	2.242	3.75	112.1
Sample 2	5	5.198	1.90	104.0
Sample 3	8	8.404	1.43	105.1

¹ Values shown were the calculated mean Cu^{2+} for each sample.

2.6. Effect of pH

The spectroscopic characters of the probe were studied in the pH range 2–13 in sodium acetate-acetic acid buffer solution. Figure 5 shows the fluorescence response of **ACP** toward Cu^{2+} in the pH range. The fluorescence intensities of the mixture were very high in the pH range 2–4, yet the fluorescence emission ($\lambda_{\text{ex}}/\lambda_{\text{em}} = 561/580 \text{ nm}$) drastically decreases in pH up to 5 and varies slightly until 11. This may be attributed to the fact that H^+ and Cu^{2+} competitively bind to **ACP** in acid solutions, consequently the formation of Cu^{2+} -**ACP** complexes are inhibited, thus the mixture displayed high fluorescence intensities in the pH range 2–4. Moreover, in the pH range 11–13 the mixture possess very high fluorescence emission, which is most probably due to the fact that in strongly alkaline solutions OH^- and **ACP** competitively bind to Cu^{2+} . The more alkaline of the buffer solution is, the more liable it is to form $\text{Cu}(\text{OH})_4^{2-}$, and the more difficult it is to form Cu^{2+} -**ACP** complexes. Therefore, the Cu^{2+} -**ACP** complexes are stable only in the pH range 6–11.

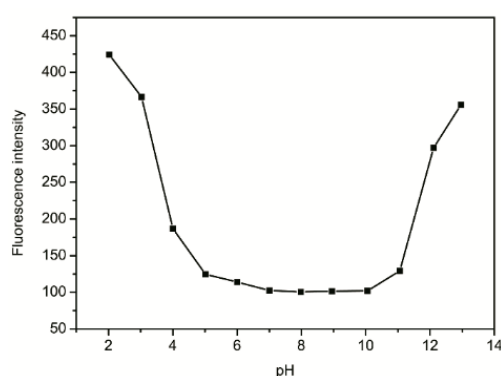


Figure 5. The effect of different pH values on the spectroscopic characteristics of Cu^{2+} -**ACP**.

2.7. Binding Mechanism

As a new kind of porphyrin, **ACP** is endowed with a cyclic π -aromatic system and exhibits unique coordination chemistry. Owing to the four pyrrole units of **ACP**, Cu^{2+} would coordinate with pyrrole N atoms in a square planar shape. We have simulated the **ACP**- Cu^{2+} complex through density functional theory (DFT) calculations with the Becke-3-Lee-Yang-Parr (B3LYP) exchange function using the Gaussian 09 package [34]. The 6-31G (d, p) basis sets were used except for Cu^{2+} , where a LANL2DZ effective core potential (ECP) was employed. Figure 6 represents the molecular geometry optimization according to the 1:1 binding stoichiometry of **ACP** with the Cu^{2+} ion. The atom distances of N1-N3 and N2-N4 in **ACP** were 4.272 and 4.115 Å (Figure 6a), respectively, yet in **ACP**- Cu^{2+} complex their distances decreased to 3.999 and 3.776 Å, respectively, which can be attributed to the fact that the electron-donating N atom of pyrrole rings have high affinity to bind to Cu^{2+} with short bond lengths (shown in Figure 6c). Moreover, the four pyrrole rings in **ACP** are almost planar, yet during the formation of **ACP**- Cu^{2+} complex, the Cu^{2+} ions occupy the coordination center of **ACP** and the molecular plane was slightly contorted and metamorphosed due to the formation of coordination bonds and steric strain (Figure 6d). According to the experimental results, the **ACP**- Cu^{2+} complex exhibits an absorption at 632 nm compared with the absorption at 660.5 for **ACP**. This can be easily explained by the above mentioned phenomena: the introduction of Cu^{2+} distorts the conjugate plane of **ACP** molecule, and to some extent destroys the conjugated π -bond of the four pyrrole rings, thus leading to a blue-shift in the UV-visible absorption spectrum of **ACP**- Cu^{2+} .

In addition, we analysed the frontier molecular orbitals (FMO's) of bare **ACP** and the **ACP**- Cu^{2+} complex. This will help us to understand the quenching phenomenon upon addition of Cu^{2+} ions. The calculated FMO's are shown in Figure 7.

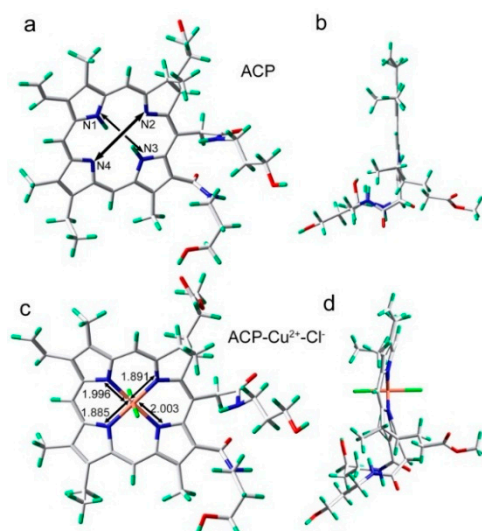


Figure 6. Energy-minimized structures by DFT calculations: (a) viewed from the front for ACP; (b) viewed from the side for ACP; (c) viewed from the front for ACP-Cu²⁺ complex; (d) viewed from the side for ACP-Cu²⁺ complex.

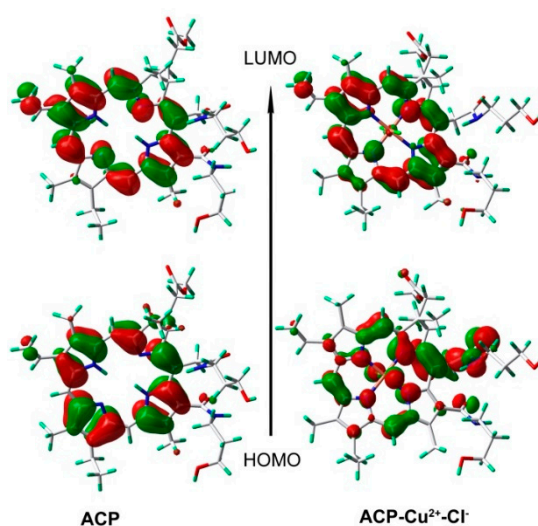


Figure 7. Frontier molecular orbitals of ACP and ACP-Cu²⁺ complex (1:1) obtained at B3LYP/6-31G(d, p) and B3LYP/LANL2DZ level, respectively.

In the absence of Cu²⁺, the solution of ACP is pale yellow and fluorescent, and from the figure it is seen that the electron density in HOMO and LUMO are both localized on the pyrrole rings, mainly involving the π - π^* electronic transitions of conjugated π -bonds. Upon the addition of Cu²⁺ into the ACP solution, the HOMO of ACP-Cu²⁺ is distributed over the pyrrole rings, Cu²⁺ and amide in the side chain, while in the LUMO the electron density is mainly localized on the pyrrole rings. This is mainly involved in the charge-transfer (CT) from Cu²⁺ and amide in the side chain to the pyrrole rings. Therefore, the quenching phenomenon may be explained by two factors: one is that the coordination of Cu²⁺ to ACP decreases the electron-donating ability of the nitrogen atoms of ACP, and to some extent the conjugated- π bond, whereby the most important ultraviolet absorption and fluorescence were destroyed, resulting in a colour change and fluorescence quenching; the other because of the paramagnetic nature of Cu²⁺. These results support our expectation that ACP could serve as a sensitive fluorescent probe as well as a naked-eye probe for Cu²⁺.

3. Experimental Section

3.1. General Information

All chemicals used in this paper were obtained from commercial suppliers and used without further purification. Ultrapure water was used for aqueous solution preparation. All samples were prepared at room temperature and promptly used for UV-Vis and fluorescence determination. Zinc chloride (98%), copper(II) chloride dihydrate (99%), nickel(II) chloride hexahydrate (98%), barium chloride (99.5%), silver nitrate (99.8%), cobalt(II) chloride hexahydrate (90%), sodium chloride (99.5%), potassium chloride (99.5%), magnesium chloride hexahydrate (98%), cadmium chloride (99%), lead(II) nitrate (99%), ferric chloride hexahydrate (99%) and calcium chloride anhydrous (96%) were obtained from Sinopharm Chemical Reagent Co. Ltd. (Shanghai, China). All the chemical reactions were performed under argon protection and away from sunshine. $^1\text{H-NMR}$ and $^{13}\text{C-NMR}$ spectra were recorded at 400 and 100 MHz, respectively, on an AMX400 spectrometer (Bruker, Bremen, Germany) with tetramethylsilane (TMS) as an internal standard. Mass spectra were recorded with a VG-7070 spectrometer (Hitachi, Manchester, UK). UV-Vis absorption and emission spectra were recorded using a UV-160A spectrophotometer (Shimadzu, Kyoto, Japan) and spectrofluorophotometer with a 150 W xenon lamp as a visible excitation light source (RF-5301PC, Shimadzu), respectively. All measurements were made at room temperature (about 25 °C). All spectra were obtained in a quartz cuvette (path length = 1 cm). The excitation and emission slit widths were both 10 nm, and PMT voltage of 700 V. The fluorescence intensities/spectra were measured at $\lambda_{\text{ex/em}} = 412/668$ nm.

3.2. General Procedure for Synthesis of the title Compound

Methyl pyropheophorbide a (Mpa) was synthesized according to the literature procedure [32]. Then propanolamine (1 mL) was added to a solution of Mpa (66.73 mg, 0.11 mmol) in chloroform and the reaction stirred under a nitrogen atmosphere for 24 h at rt. The reaction mixture was then concentrated, and the residue was dispersed in dichloromethane (30 mL), and then washed by water (30 mL) for three times. After drying and evaporation of the solvent, the residue was purified by silica gel chromatography with methanol: dichloromethane (1:15) as the eluent to give pure **ACP** (76%). $^1\text{H-NMR}$ (CDCl_3) δ (ppm): 1.00~1.10 (m, 2H, 13^4-CH_2), 1.26~1.28 (m, 2H, 15^5-CH_2), 1.67 (t, $J = 7.6$ Hz, 3H, 8^2-CH_3), 1.68 (d, $J = 7.2$ Hz, 3H, 18- CH_3), 1.73~1.81 (m, 2H, 15^4-CH_2), 1.86~1.91 (b, 2H, 13^3-CH_2), 2.22~2.28 (m, 2H, 172- CH_2), 2.41~2.45 (m, 2H, 17^1-CH_2), 3.27 (s, 3H, 7- CH_3), 3.48 (s, 3H, 2- CH_3), 3.51 (s, 3H, 12- CH_3), 3.68 (s, 3H, 17^3-OCH_3), 3.72 (q, $J = 3.76$ Hz, 2H, 8^1-CH_2), 3.75~3.88 (m, 4H, 13^5-CH_2 , 15^6-CH_2), 4.31 (b, 1H, 17-H), 4.35 (q, $J = 7.2$ Hz, 1H, 18-H), 4.46 (d, $J = 7.2$ Hz, 3H, 18- CH_3), 5.29 (d, $J = 18.5$ Hz, 1H, 15-H), 5.39 (d, $J = 18.5$ Hz, 1H, 15-H), 6.13 (d, $J = 2.8$ Hz, 1H, 3^2-H (Z)), 6.33 (d, $J = 2.8$ Hz, 1H, 3^2-H (E)), 7.32 (bs, 1H, 13^2-NH), 8.09 (dd, $J_1 = 6.0$ Hz, $J_2 = 11.6$ Hz, 1H 3^1-H), 8.81 (s, 1H, 20-H), 9.62 (s, 1H, 10-H), 9.64 (s, 1H, 5-H); $^{13}\text{C-NMR}$ (MeOD) δ (ppm): 10.0, 11.5, 11.8, 17.8, 19.8, 23.5, 29.5, 31.8, 32.0, 33.2, 33.3, 33.9, 37.4, 38.6, 38.8, 50.4, 52.8, 54.4, 56.0, 60.4, 60.9, 70.5, 94.7, 98.9, 101.8, 103.5, 121.2, 129.5, 130.5, 130.9, 135.1, 135.6, 136.1, 136.8, 139.6, 145.3, 149.8, 154.8, 171.8, 175.1, 175.2. Anal calcd for $\text{C}_{41}\text{H}_{52}\text{N}_6\text{O}_6$: C 67.93, H 7.23, N 11.59; found C 67.78, H 7.46, N 11.28.

4. Conclusions

In summary, we have prepared **ACP**, a simple but effective colorimetric and fluorescent probe for Cu^{2+} detection, from methyl pheophorbide-a. It shows excellent sensitivity and selectivity for Cu^{2+} over other common metal ions in aqueous media. More importantly, the color change upon the addition of Cu^{2+} to **ACP** solutions could make it a suitable "naked eye" indicator for Cu^{2+} . Meanwhile, our study of the fluorescence quenching of **ACP-Cu** $^{2+}$ complex showed the detection limit was 7.5×10^{-8} mol/L, which suggested that **ACP** can act as a highly sensitive probe for Cu^{2+} and can be used to quantitatively detect low levels of Cu^{2+} in aqueous solution.

Acknowledgments: This work was supported by the National Nature Science Foundation of China (No. 20972036, 21272048) and the Program for Scientific Technological Innovation Team Construction in Universities of Heilongjiang Province (No. 211TD010). The theoretical calculations were conducted on the ScGrid and Deepcomp7000 the Supercomputing Center, Computer Network Information Center of Chinese Academy of Sciences.

Author Contributions: Yingxue Jin and Zhiqiang Wang conceived and designed the experiments; Guohua Zhu and Wenting Li performed the experiments; Guohua Zhu and Jinghua Li analyzed the data; Yingxue Jin contributed reagents/materials/analysis tools; Zhiqiang Wang wrote the paper.

Conflicts of Interest: The authors declare no conflict of interest.

References

1. Quang, D.T.; Kim, J.S. Fluoro- and chromogenic chemodosimeters for heavy metal ion detection in solution and biospecimens. *Chem. Rev.* **2010**, *110*, 6280–6301. [[CrossRef](#)] [[PubMed](#)]
2. Duffus, J.H. “Heavy metals” a meaningless term? (IUPAC Technical Report). *Pure Appl. Chem.* **2002**, *74*, 793–807. [[CrossRef](#)]
3. Malvankar, P.L.; Shinde, V.M. *N,N*-dibromodiethylbarbituric acid as an analytical reagent. Part 1. Determination of some pharmaceutically important hydrazine derivatives. *Analyst* **1991**, *116*, 1081–1085. [[CrossRef](#)] [[PubMed](#)]
4. Malik, A. Metal bioremediation through growing cells. *Environ. Int.* **2004**, *30*, 261–278. [[CrossRef](#)] [[PubMed](#)]
5. Fatemi, N.; Sarkar, B. Molecular mechanism of copper transport in Wilson disease. *Environ. Health Perspect.* **2002**, *110*, 695–698. [[CrossRef](#)] [[PubMed](#)]
6. Gaggelli, E.; Kozłowski, H.; Valensin, D.; Valensin, G. Copper homeostasis and neurodegenerative disorders (Alzheimer’s, prion, and Parkinson’s diseases and amyotrophic lateral sclerosis). *Chem. Rev.* **2006**, *106*, 1995–2044. [[CrossRef](#)] [[PubMed](#)]
7. Lovell, M.A.; Robertson, J.D.; Teesdale, W.J.; Campbell, J.L.; Markesbery, W.R. Copper, iron and zinc in Alzheimer’s disease senile plaques. *J. Neurol. Sci.* **1998**, *158*, 47–52. [[CrossRef](#)]
8. Säbel, C.E.; Neureuther, J.M.; Siemann, S. A spectrophotometric method for the determination of zinc, copper, and cobalt ions in metalloproteins using Zincon. *Anal. Biochem.* **2010**, *397*, 218–226. [[CrossRef](#)] [[PubMed](#)]
9. Yamini, Y.; Tamaddon, A. Solid-phase extraction and spectrophotometric determination of trace amounts of copper in water samples. *Talanta* **1999**, *49*, 119–124. [[CrossRef](#)]
10. DeWitt, R.; Watters, J.I. Spectrophotometric investigation of a mixed complex of copper(II) ion with oxalate ion and ethylenediamine. *J. Am. Chem. Soc.* **1954**, *76*, 3810–3814. [[CrossRef](#)]
11. Grujicic, D.; Pesic, B. Electrodeposition of copper: the nucleation mechanisms. *Electrochim. Acta* **2002**, *47*, 2901–2912. [[CrossRef](#)]
12. Bond, A.M.; Wallace, G.G. Simultaneous determination of copper, nickel, cobalt, chromium(VI), and chromium(III) by liquid chromatography with electrochemical detection. *Anal. Chem.* **1982**, *54*, 1706–1712. [[CrossRef](#)]
13. Etienne, A. Electrochemical method to measure the copper ionic diffusivity in a copper sulfide scale electrochemical science—Technical papers. *J. Electrochem. Soc.* **1970**, *117*, 870–874. [[CrossRef](#)]
14. Otero, R.J.; Moreda, P.A.; Bermejo, B.A.; Bermejo, B.P. Evaluation of commercial C18 cartridges for trace elements solid phase extraction from seawater followed by inductively coupled plasma-optical emission spectrometry determination. *Anal. Chim. Acta* **2005**, *536*, 213–218. [[CrossRef](#)]
15. Rao, K.S.; Balaji, T.; Rao, T.P.; Babu, Y.; Naidu, G.R.K. Determination of iron, cobalt, nickel, manganese, zinc, copper, cadmium and lead in human hair by inductively coupled plasma-atomic emission spectrometry. *Spectrochim. Acta B* **2002**, *57*, 1333–1338.
16. Murillo, M.; Benzo, Z.; Marciano, E.; Gomez, C.; Garaboto, A.; Marin, C. Determination of copper, iron and nickel in edible oils using emulsified solutions by ICP-AES. *J. Anal. At. Spectrom.* **1999**, *14*, 815–820. [[CrossRef](#)]
17. Rahil-Khazen, R.; Bolann, B.J.; Myking, A.; Ulvik, R.J. Multi-element analysis of trace element levels in human autopsy tissues by using inductively coupled atomic emission spectrometry technique (ICP-AES). *J. Trace Elem. Med. Biol.* **2002**, *16*, 15–25. [[CrossRef](#)]

18. Pourreza, N.; Hoveizavi, R. Simultaneous preconcentration of Cu, Fe and Pb as methylthymol blue complexes on naphthalene adsorbent and flame atomic absorption determination. *Anal. Chim. Acta* **2005**, *549*, 124–128. [[CrossRef](#)]
19. Ghaedi, M.; Ahmadi, F.; Shokrollahi, A. Simultaneous preconcentration and determination of copper, nickel, cobalt and lead ions content by flame atomic absorption spectrometry. *J. Hazard. Mater.* **2007**, *142*, 272–278. [[CrossRef](#)] [[PubMed](#)]
20. Aksuner, N.; Henden, E.; Yilmaz, I.; Cukurovali, A. A highly sensitive and selective fluorescent sensor for the determination of copper(II) based on a schiff base. *Dyes Pigments* **2009**, *83*, 211–217. [[CrossRef](#)]
21. Li, Y.; Zhang, X.; Zhu, B.; Xue, J.; Zhu, Z.; Tan, W. A simple but highly sensitive and selective colorimetric and fluorescent probe for Cu²⁺ in aqueous media. *Analyst* **2011**, *136*, 1124–1128. [[CrossRef](#)] [[PubMed](#)]
22. Shao, N.; Zhang, Y.; Cheung, S.M.; Yang, R.H.; Chan, W.H.; Mo, T.; Li, K.A.; Liu, F. Copper ion-selective fluorescent sensor based on the inner filter effect using a spiropyran derivative. *Anal. Chem.* **2005**, *77*, 7294–7303. [[CrossRef](#)] [[PubMed](#)]
23. Dujols, V.; Ford, F.; Czarnik, A.W. A long-wavelength fluorescent chemodosimeter selective for Cu²⁺ ion in water. *J. Am. Chem. Soc.* **1997**, *119*, 7386–7387. [[CrossRef](#)]
24. Kumar, M.; Kumar, N.; Bhalla, V.; Sharma, P.R.; Kaur, T. Highly Selective fluorescence turn-on chemodosimeter based on rhodamine for nanomolar detection of copper ions. *Org. Lett.* **2012**, *14*, 406–409. [[CrossRef](#)] [[PubMed](#)]
25. Nose, K.; Fujita, H.; Omata, T. Chemical role of amines in the colloidal synthesis of CaSe quantum dots and their luminescence properties. *Luminescence* **2007**, *126*, 21–26.
26. Chen, Y.F.; Rosenzweig, Z. Luminescent Cds quantum dots as selective ion probes. *Anal. Chem.* **2002**, *74*, 5132–5138. [[CrossRef](#)] [[PubMed](#)]
27. Lee, M.H.; Kim, H.; Yoon, S.; Park, N.; Kim, J.S. Metal ion induced FRET OFF-ON in tren/dansyl-appended rhodamine. *Org. Lett.* **2008**, *10*, 213–216. [[CrossRef](#)] [[PubMed](#)]
28. Emaus, R.K.; Grunwald, R.; Lemasters, J.J. Rhodamine 123 as a probe of transmembrane potential in isolated rat-liver mitochondria: Spectral and metabolic properties. *Biochim. Biophys. Acta Bioenerg.* **1986**, *850*, 436–448. [[CrossRef](#)]
29. Gaponik, N.; Talapin, D.V.; Rogach, A.L.; Hoppe, K.; Shevchenko, E.V.; Kornowski, A.; Eychmuller, A.; Weller, H. Thiol-capping of CaTe nanocrystals: An alternative to organometallic synthetic routes. *J. Phys. Chem. B* **2002**, *106*, 7177–7185.
30. Luo, H.-Y.; Zhang, X.-B.; Jiang, J.-H.; Li, C.-Y.; Peng, J.; Shen, G.-L.; Yu, R.-Q. An optode sensor for Cu²⁺ with high selectivity based on porphyrin derivative appended with bipyridine. *Anal. Sci.* **2007**, *23*, 551–555. [[CrossRef](#)] [[PubMed](#)]
31. Ghosh, I.; Saleh, N.; Nau, W.M. Selective time-resolved binding of copper(II) by pyropheophorbide-amethyl ester. *Photochem. Photobiol. Sci.* **2010**, *9*, 649–654. [[CrossRef](#)] [[PubMed](#)]
32. Wang, J.-J.; Ji, W.-Y.; Han, G.-F.; Wu, X.-R.; Wang, L.M.; Shen, R.J. Synthesis of 3-alkyloyl-3-devinyl-methyl pyropheophorbide-a and the effect of the peripheral carbonyl groups on the ¹H-NMR and the visible spectra. *Acta Chim. Sin.* **2004**, *62*, 302–311.
33. Caballero, A.; Espinosa, A.; Tafraga, A.; Molina, P. Ferrocene-based small molecules for dual-channel sensing of heavy- and transition-metal cations. *J. Org. Chem.* **2008**, *73*, 5489–5497. [[CrossRef](#)] [[PubMed](#)]
34. Frisch, M.J.; Trucks, G.W.; Schlegel, H.B.; Scuseria, G.E.; Robb, M.A.; Cheeseman, J.R.; Scalmani, G.; Barone, V.; Mennucci, B.; Petersson, G.A.; et al. *Gaussian 09, Revision C.01*; Gaussian, Inc.: Wallingford, CT, USA, 2010.

Sample Availability: Samples of the compound ACP are available from the authors.



© 2016 by the authors; licensee MDPI, Basel, Switzerland. This article is an open access article distributed under the terms and conditions of the Creative Commons by Attribution (CC-BY) license (<http://creativecommons.org/licenses/by/4.0/>).